HHS Public Access

Author manuscript

Oncogene. Author manuscript; available in PMC 2022 June 01.

Published in final edited form as:

Oncogene. 2021 December ; 40(49): 6653–6665. doi:10.1038/s41388-021-02057-0.

Induction of SREBP1 degradation coupled with suppression of SREBP1-mediated lipogenesis impacts the response of EGFR mutant NSCLC cells to osimertinib

Zhen Chen[1], **Danlei Yu**[1], **Taofeek K. Owonikoko**[2], **Suresh S. Ramalingam**[1], **Shi-Yong Sun**[1,*]

[1]Department of Hematology and Medical Oncology, Emory University School of Medicine and Winship Cancer Institute, Atlanta, GA, USA

[2]Department of Medicine, University of Pittsburgh and Hillman Cancer Center, Pittsburgh, PA, USA.

Abstract

Emergence of acquired resistance to osimertinib (AZD9291), the first-approved third generation EGFR inhibitor that selectively and irreversibly inhibits the activating EGFR mutations and the resistant T790M mutation, is a giant and urgent clinical challenge. Fully understanding the biology underlying the response of EGFR mutant non-small cell lung cancer (NSCLC) to osimertinib is the foundation for development of mechanism-driven strategies to overcome acquired resistance to osimertinib or other third generation EGFR inhibitors. This study focused on tackling this important issue by elucidating the critical role of sterol regulatory element-binding protein 1 (SREBP1) degradation in conferring the response of EGFR mutant NSCLC cells to osimertinib and by validating the strategy via directly targeting SREBP1 for overcoming osimertinib acquired resistance. Osimertinib facilitated degradation of the mature form of SREBP1 (mSREBP1) in a GSK3/FBXW7-dependent manner and reduced protein levels of its regulated genes in EGFR-mutant NSCLC cells/tumors accompanied with suppression of lipogenesis. Once resistant, EGFR-mutant NSCLC cell lines possessed elevated levels of mSREBP1, which were resistant to osimertinib modulation. Both genetic and pharmacological inhibition of SREBP1 sensitized osimertinib-resistant cells and tumors to osimertinib primarily through enhancing Bim-dependent induction of apoptosis, whereas enforced expression of ectopic SREBP1 in sensitive EGFR-mutant NSCLC cells compromised osimertinib's cell-killing effects. Collectively, we have demonstrated a novel connection between osimertinib and SREBP1 degradation and its impact on

*Correspondence: Shi-Yong Sun, Ph.D., Department of Hematology and Medical Oncology, Emory University School of Medicine and Winship Cancer Institute, 1365-C Clifton Road, C3088, Atlanta, GA 30322. Phone: (404) 778-2170; Fax: (404) 778-5520; ssun@emory.edu.

Author Contributions

Conceptualization: S-Y.S., Z.C., T.K.O. and S.S.R.
Investigation: Z.C. and D.Y.
Methodology: Z.C. and S-Y.S.
Writing/Original Draft: Z.C. and S-Y.S.
Funding Acquisition: S-Y.S. and S.S.R.
Supervision: T.K.O, S.S.R and S-Y.S.

Competing interest statement

S.S.R. is on consulting/advisory board for AstraZeneca, Amgen, BMS, Merck, Roche, Tesaro and Amgen. T.K.O. is on consulting/advisory board for Novartis, Celgene, Lilly, Sandoz, Abbvie, Eisai, Takeda, Bristol-Myers Squibb, MedImmune, Amgen, AstraZeneca and Boehringer Ingelheim. Other authors declare that they have no conflict of interest.

the response of EGFR mutant NSCLC cells to osimertinib and suggested an effective strategy for overcoming acquired resistance to osimertinib, and possibly other EGFR inhibitors, via targeting SREBP1.

Keywords

SREBP1; EGFR; osimertinib; resistance; non-small cell lung cancer

Introduction

Lung cancer consists of 80% non-small cell lung cancer (NSCLC) and is the leading cause of cancer-related deaths worldwide[1, 2]. The treatment of NSCLC has evolved to a great extent due to the discovery of epidermal growth factor receptor (EGFR) activating mutations as an effective therapeutic target. The first generation EGFR-tyrosine kinase inhibitors (EGFR-TKIs; e.g., gefitinib and erlotinib) and second generation EGFR-TKIs (e.g., afatinib) have achieved great success in benefiting patients[3]. Unfortunately, patients receiving these EGFR-TKIs ultimately develop disease progression due to acquired resistance with the most common mechanism being the T790M mutation[4]. Osimertinib (AZD9291 or TAGRISSO™), as a representative and the first-approved third generation EGFR-TKI, selectively and irreversibly inhibits the activating EGFR mutations and the resistant T790M mutation while sparing wild-type (WT) EGFR and is used for the treatment of T790M-positive patients as a second-line therapy and for the treatment of advanced lung cancer carrying activating EGFR mutations, regardless of T790M mutation status as a first-line therapy[4]. However, patients still inevitably develop acquired resistance to this treatment, limiting its long-term efficacy. Therefore, it is urgent and clinically desirable to explore the underlying resistance mechanisms and develop effective therapies to overcome acquired resistance to osimertinib.

One of the hallmarks of cancer is lipid metabolism reprogramming. Cancer cells exhibit significant metabolic alterations to support cell proliferation. Unlike normal cells that rely mainly on the uptake of exogenous fatty acids, cancer cells increase the rate of *de novo* synthesis, which is important for membrane biosynthesis, energy production and protein modification[5, 6]. Accumulating evidence has demonstrated that lipogenesis is elevated in human cancers. Meanwhile, lipid uptake and storage is also increased in tumors[5, 7, 8]. Sterol regulatory element-binding proteins (SREBPs), a family of membrane-bound transcription factors, play a key role in regulating lipid metabolism. Three forms of SREBPs (SREBP1-a, SREBP1-c and SREBP2) are encoded by the genes SREBF1 and SREBF2. SREBP1 is mainly involved in the regulation of fatty acid synthesis, phospholipid and triacylglycerol synthesis, while SREBP2 primarily regulates cholesterol synthesis[9, 10]. When cellular sterol levels are sufficient, SREBP1 is located in the endoplasmic reticulum (ER) and associated with SREBP-cleavage activating protein (SCAP). Once sterol levels drop, SREBP1 is cleaved by site-1 and site-2 proteases (S1P and S2P) in the Golgi, and released as a mature form of the N-terminal protein (mSREBP1), which is translocated to the nucleus where it activates transcription of lipogenesis genes and low density lipoprotein receptor[9, 11]. It has been shown that SREBP1 is highly activated in cancers, and that genetic and

pharmacological targeting of SREBP1 significantly inhibited tumor growth[12], suggesting that SREBP1 might be a novel target in cancer.

Toward our effort to thoroughly understand the molecular mechanisms of osimertinib against EGFRm NSCLC cells, we have identified a previously unrevealed connection between mSREBP1 modulation including its mediated lipid metabolism and osimertinib-mediated targeted cancer therapy. In this study, we have demonstrated that osimertinib dramatically decreases the levels of mSREBP1 and its targeted proteins including fatty-acid synthase (FASN) and acetyl-CoA carboxylase (ACC) in EGFRm NSCLC cell lines primarily through enhancing GSK3/FBXW7-mediated mSREBP1 degradation. Osimertinib loses its ability to decrease the levels of mSREBP1, FASN and ACC and to suppress lipid metabolism in EGFRm NSCLC cell lines with osimertinib acquired resistance possessing elevated mSREBP1. Targeting SREBP1 with both genetic and pharmacological approaches restores the responses of osimertinib-resistant cells and tumors to osimertinib *in vitro* and *in vivo*, suggesting a possible therapeutic avenue for overcoming acquired resistance to osimertinib and possibly other third generation EGFR-TKIs.

Results

Osimertinib inhibits mTOR complex 2 (mTORC2) signaling and decreases mSREBP1 levels in EGFRm NSCLC cells.

We previously documented that osimertinib effectively suppresses MEK/ERK signaling with the induction of apoptosis through modulation of Bim and Mcl-1 degradation[13]. We then checked whether osimertinib affects PI3K/Akt, another important signaling pathway downstream of EGFR[14], in EGFRm NSCLC cells. Intriguingly, osimertinib effectively deceased the levels of not only p-Akt (S473), but also p-Akt (T450) and p-NDRG1 (T346), which all serve as substrates of mTORC2[15], in the two EGFRm NSCLC cell lines, PC-9 and HCC827 (Fig. 1A), suggesting that osimertinib inhibits mTORC2 signaling. Given that mTORC2 stabilizes mSREBP1 via inhibiting its degradation[16], we then logically questioned whether the mutation-selective EGFR-TKI, osimertinib, decreases mSREBP1 levels in sensitive EGFRm NSCLC cell lines. Indeed, we observed concentration-dependent and time-dependent reduction of mSREBP1, ACC and FASN with minimal decrease of precursor SREBP1 in EGFRm cell lines (Figs. 1B and C), but not in cell lines with WT EGFR exposed to osimertinib (Fig. 1B). We noted that mSREBP1 in H596 cells was more condensed and migrated a little bit faster than those in H1299 and A549 cell lines. This may be caused by different post-translation modifications of mSREBP proteins. Nonetheless, osimertinib does not decrease the levels of mSREBP1 in these cell lines. Interestingly, other EGFR-TKIs, including the 1st generation EGFR-TKI, erlotinib, the 2nd generation EGFR-TKI, afatinib, and the 3rd generation EGFR-TKIs, EGF816 and CO1686, all effectively decreased the levels of mSREBP1, ACC and FASN in HCC827 and PC-9 cells (Fig. 1D). Immunofluorescence (IF) further confirmed that, in both HCC827 and PC-9 cells, osimertinib significantly reduced FASN and ACC levels (Fig. 1E). In osimertinib-treated PC-9 xenograft tumors, decreased FASN was also detected in comparison with vehicle-treated tumor tissue (Fig. 1F). These results together clearly indicate that osimertinib and

other EGFR-TKIs effectively decrease mSREBP1 levels and its regulated proteins primarily in EGFRm NSCLC cells.

Osimertinib effectively suppresses SREBP1-regulated lipid metabolism in EGFRm NSCLC cells.

Since the mSREBP/ACC/FASN axis critically regulates lipid metabolism, particularly fatty acid synthesis, phospholipid and triacylglycerol synthesis[9, 17], we next determined whether osimertinib accordingly alters lipid metabolism in EGFRm NSCLC cells. In both HCC827 and PC-9 cells, osimertinib substantially reduced lipid droplets as detected by Nile Red staining (Fig. 2A). In PC-9 xenograft tumors receiving osimertinib treatment, lipid droplets were also dramatically reduced using both Nile Red staining (Fig. 1F) and Oil Red O staining (Fig. 2B). Therefore, it appears that osimertinib inhibits lipid metabolism in EGFRm NSCLC cells and tumors. Furthermore, we conducted an untargeted lipidomic analysis in HCC827 cells treated with DMSO and osimertinib, respectively. Unsupervised hierarchical clustering separated the cells exposed to osimertinib from the DMSO-treated cells, based on the distinct profiles of 148 lipid metabolites (Fig. 2C and supplementary Fig. S1A). Out of the 148 lipid metabolites, 50 of them were significantly (false discovery rate, FDR < 0.05) altered when treated with osimertinib (Fig. 2D and Fig. S2). Lipid classes of triacylglycerol (TAG), diacylglycerol (DAG), sphingomyelin (SM), ceramide (CER) and phosphatidylethanolamine (PE), especially polyunsaturated fatty acids phosphatidylethanolamine (PUFA PE), were significantly decreased in cells treated with osimertinib (Fig. 2E and Fig. S1B). The phosphatidylcholine (PC) class showed diverse but not significant changes in cells treated with osimertinib (Fig. S1C). These results thus confirm that osimertinib effectively suppresses metabolism of lipids, particularly those regulated by SREBP1, in EGFRm NSCLC cells.

Osimertinib reduces mSREBP1 levels through facilitating GSK3/FBXW7-mediated mSREBP1 degradation.

Considering that mTORC2 inhibition induces GSK3/FBXW7-mediated proteasomal degradation of mSREBP1[16], we then determined whether osimertinib decreases mSREBP1 levels through modulating its degradation. We found that the presence of MG132, a widely used proteasome inhibitor, not only enhanced the basal levels of mSREBP1, but also rescued mSREBP1 reduction induced by osimertinib in PC-9, HCC827 and H1975 cells (Fig. 3A). The cycloheximide (CHX) chase assay showed that mSREBP1 was degraded more rapidly in osimertinib-treated PC-9 and HCC827 cells than in their corresponding DMSO-treated cells (Figs. 3B and 3C). These findings collectively indicate that osimertinib destabilizes mSREBP1 by promoting proteasomal degradation. Moreover, we determined whether osimertinib alters SREBP1 mRNA expression in EGFRm NSCLC cells and found that osimertinib did not alter SREBP1 mRNA expression in both PC-9 and HCC827 cells (Fig. S3)

We next determined whether GSK3/FBXW7 is involved in osimertinib-induced mSREBP1 degradation. We found that osimertinib reduced mSREBP1 levels in the absence of a GSK3 inhibitor (CHIR99021 or SB216763), but did not do so in the presence of these GSK3 inhibitors (Fig. 3D). In agreement, silencing GSK3 with a specific small interfering RNA

(siRNA) also rescued mSREBP1 reduction induced by osimertinib in PC-9 and HCC827 cells (Fig. 3E). Furthermore, knockdown of FBXW7 with a siRNA or small hairpin RNA (shRNA) enhanced the basal level of mSREBP1 and rescued mSREBP1 reduction induced by osimertinib in these cell lines (Figs. 3F and 3G). Taken together, these results demonstrate that osimertinib promotes GSK3/FBXW7-mediated mSREBP1 degradation.

EGFRm NSCLC cells with osimertinib acquired resistance and NSCLC tissues relapsed from EGFR-TKI treatment possess elevated levels of mSREBP1 and FASN, which are resistant to osimertinib modulation.

To explore whether the acquired osimertinib resistance is related to dysregulation of SREBP1-dependent lipid metabolism, we then compared the basal levels of mSREBP1 between PC-9 and HCC827 parental cell lines and their derived osimertinib-resistant cell lines including PC-9/AR(osimertinib-resistant with unknown mechanisms), PC-9/GR/AR (gefitinib- and osimertinib-resistant with T790M mutation), PC-9/3M (19del, T790M and C797S triple mutations) and HCC827/AR (osimertinib-resistant with *MET* amplification). As shown in Fig. 4A, the basal levels of mSREBP1, ACC and FASN were higher in these resistant cell lines than their corresponding parental cell lines. Importantly, we detected minimal or no reduction of mSREBP1, ACC and FASN in the resistant cell lines when treated with osimertinib (Figs. 4B and 4C). Moreover, IF staining also showed that both FASN levels and lipid droplets were reduced with osimertinib treatment in PC-9 and HCC827 cells, but not in their corresponding resistant cell lines (Fig. 4D and S4). Hence, osimertinib loses its ability to reduce mSREBP1 levels and to inhibit its regulated lipid metabolism in cells with osimertinib acquired resistance.

We also analyzed paired NSCLC tissues from 46 patients before EGFR-TKI (first generation) treatment (baseline) and after relapse. Given the unavailability of antibody specifically recognizing mSREBP1 that can be used in immunohistochemistry (IHC), we alternatively detected FASN expression in these tissue with IHC and found that FASN levels were significantly increased in relapsed tissues compared with those in tissues before the treatment (Fig. 4E), confirming the elevation of SREBP1/FASN axis in the relapsed tissues. Among 46 patients, 38 patients partially responded to EGRF-TKI treatment (partial response; PR), whereas 8 patients were not responsive (stable disease; SD). FASN expression was significantly higher in patients with SD than in patients with PR (Fig. 4F), suggesting that tumors with highly elevated SREBP1/FASN axis may respond poorly to EGFR-TKI treatment.

Enforced expression of ectopic SREBP1 in sensitive EGFRm NSCLC cell lines confers cell resistance to osimertinib.

To determine whether SREBP1 elevation is associated with development of acquired resistance to osimertinib, we enforced elevation of SREBP1 levels in the sensitive EGFRm NSCLC cell lines, PC-9 and HCC827, through expressing ectopic SREBP1 as demonstrated in Fig. 4G and then examined its impact on cell responses to osimertinib. Both cell lines expressing ectopic SREBP1 were much more resistant than their corresponding parental cell lines to osimertinib as evaluated by measuring both cell survival (Fig. 4H) and apoptosis

(Figs. 4G and 4I). Hence, it is clear that enforced SREBP1 expression in sensitive EGFRm NSCLC cells confers resistance to osimertinib.

Genetic knockdown of SREBP1 reverses osimertinib resistance *in vitro* and *in vivo*.

The elevation of mSREBP1/FASN in osimertinib-resistant cell lines and their unresponsiveness to osimertinib treatment as demonstrated above plus the protective effect of enforced expression of ectopic SREBP1 in the sensitive EGFRm NSCLC cells on osimertinib-induced cell-killing suggest a critical role of SREBP1 in development of acquired resistance to osimertinib. If so, we anticipated that suppression of mSREBP1 should re-sensitize the resistant cells to osimertinib treatment. To this end, we first tested the impact of genetic knockdown of SREBP1 on sensitivities of osimertinib-resistant cell lines to osimertinib. We found that siRNA-mediated knockdown of SREBP1 including mSREBP1, which was confirmed by Western blotting (Fig. 5A), effectively enhanced the effects of osimertinib on inducing cleavage of PARP and caspase-3 (Fig. 5A) and on increasing annexin-V-positive cells (Fig. 5B) in both PC-9/AR and HCC827/AR cells. Similarly, both transient and stable knockdown of SREBP1 by using a shRNA in both PC-9/AR and HCC827/AR cell lines also enhanced the ability of osimertinib to reduce ACC levels (Fig. 5C), decrease cell survival (Fig. 5D), induce cleavage of PARP and caspase-3 (Fig. S5A) and increase apoptotic cells (Fig. 5E and S5B).

Moreover, we conducted an *in vivo* study to test the impact of SREBP1 knockdown on the response of osimertinib-resistant tumors to osimertinib. We found that osimertinib significantly inhibited the growth of PC-9/AR-shSREBP1 tumors, while it had minimal effect on the growth of PC-9/AR-pLKO.1 tumors (Figs. 5F–5H). Meanwhile, there were no differences in body weights between control and osimertinib groups (Figs. S6A). IHC showed that both ACC and FASN expression were significantly decreased in the PC-9/AR-shSREBP1 tumors receiving osimertinib treatment; but not in PC-9/AR-pLKO.1 tumors treated with osimertinib (Fig. S6B). Furthermore, IF staining showed that the amounts of lipid droplets and FASN expression levels were reduced in PC-9/AR-shSREBP1 tumors receiving osimertinib treatment, but not in osimertinib-treated PC-9/AR-pLKO.1 tumors (Fig. 5I).

Therefore, these *in vitro* and *in vivo* results convincingly demonstrate that enforced suppression of SREBP1 via genetic gene knockdown re-sensitizes osimertinib-resistant cells and tumors to osimertinib, suggesting targeting SREBP1/ACC/FASN-mediated lipid metabolism as an effective strategy to reverse acquired resistance to osimertinib.

Chemical inhibition of SREBP1 combined with osimertinib synergistically decreases the survival of osimertinib-resistant NSCLC cells with enhanced apoptosis and overcomes osimertinib resistance *in vivo*.

To better translate our findings to the clinical treatment of cancer in the future, we used small molecule SREBP1 inhibitors in combination with osimertinib to overcome osimertinib acquired resistance. Two SREBP1 inhibitors, PF429242 and betulin[10], when combined with osimertinib, respectively, synergistically decreased the survival of osimertinib-resistant cells (PC-9/AR and HCC827/AR) with combination indexes (CIs) < 1 (Figs. 6A and S7A).

The colony formation assay clearly showed that these combinations were significantly more potent than either agent alone in suppressing colony formation and growth of both PC-9/AR and HCC827/AR cells (Figs. 6B and S7B). Observation of morphological change showed that the combination of osimertinib and PF429242 enhanced cell detachment, a typical apoptotic phenotype (Fig. 6C). Indeed, compared with each single agent treatment, the combination of osimertinib with either PF429242 or betulin significantly enhanced apoptosis, as indicated by increased annexin V-positive cells (Figs. 6D and S7C) and cleavage of PARP and caspase-3 (Figs. 6E and S7D). Moreover, IF staining further showed that the combination of osimertinib and PF429242 dramatically reduced the formation of lipid droplets (Nile Red staining) and the levels of FASN in both PC-9/AR and HCC827/AR cells (Fig. S8). Hence, it is clear that osimertinib combined with a small molecule SREBP1 inhibitor enhances induction of apoptosis and inhibition of lipid metabolism in osimertinib-resistant cells.

Following these *in vitro* studies, we validated the efficacy of the osimertinib and PF429242 combination in suppressing the growth of osimertinib-resistant xenografts *in vivo*. While osimertinib or PF429242 alone had a minimal effect on inhibiting the growth of PC-9/AR tumors, their combination significantly reduced the growth of these tumors based on both tumor sizes and weights (Figs. 6F–H). The combination did not apparently alter mouse body weights (Fig. S9A). Thus, this combination effectively inhibits the growth of osimertinib-resistant tumors *in vivo* with well-tolerated safety, indicating its safety and efficacy in overcoming osimertinib acquired resistance.

We also detected FASN expression and lipid droplets using IF staining in these tumors and found that both FASN and Nile Red staining (lipid droplets) were clearly reduced in tumors treated with the combination in comparison with single agent-treated tumors (Fig 6I). Oil Red staining also generated similar results regarding the reduction of lipid droplets (Fig. S9B). With IHC, we also detected that both ACC and FASN levels were much lower in tumors receiving the combination treatment in those treated with either agent alone (Fig. S9C). Hence, the combination effectively inhibits the SREBP1/ACC/FASN axis and lipid metabolism in osimertinib-resistant tumors.

Osimertinib combined with SREBP1 inhibition enhances Bim-dependent apoptosis in osimertinib-resistant cells.

Our previous study demonstrated that modulation of Bim and Mcl-1 is a key mechanism for osimertinib to induce apoptosis in EGFRm NSCLC cells[13]. To understand the mechanism by which osimertinib combined with SREBP1 inhibition enhances apoptosis in osimertinib-resistant cells, we determined the effects of osimertinib and PF429242 on modulation of Bim and Mcl-1 in osimertinib-resistant cell lines. As presented in Fig. 7A, the combination of osimertinib and PF429242 increased the levels of not only Bim, but also Mcl-1 in both PC-9/AR and HCC827/AR cell lines, whereas each single agent alone did not or minimally elevated the levels of these proteins. Consistently, osimertinib apparently increased the levels of Bim and Mcl-1 in the two resistant cell lines in which SREBP1 was knocked down, but weakly in the corresponding pLKO.1 control cells (Fig. 7B). Thus, it is clear that SREBP1 inhibition in combination with osimertinib enhances elevation of both Bim and Mcl-1

levels in osimertinib-resistant cell lines. In agreement with these *in vitro* findings, increased levels of Bim, Mcl-1 and PARP cleavage were detected with Western blotting in PC-9/AR tumors treated with osimertinib and PF429242 combination in comparison with tumors receiving single agent treatment and in PC-9/AR-shSREBP1 tumors compared with PC-9/AR-pLKO.1 tumors receiving osimertinib treatment (Figs. 7C and D). With IHC, we further confirmed the enhanced Bim elevation and PARP cleavage in PC-9/AR tumors receiving osimertinib and PF429242 co-treatment (Fig. 7E) and in PC-9/AR-SREBP1 treated with osimertinib (Fig. 7F). Thus, SREBP1 inhibition combined with osimertinib clearly enhances Bim elevation with augmented induction of apoptosis *in vivo* in osimertinib-resistant tumors, despite the elevation of Mcl-1 levels.

Following these findings, we further determined whether Bim elevation plays a key role in enhancing apoptosis by osimertinib and PF429242 combination in osimertinib-resistant cells. To this end, we knocked out Bim in both PC-9/AR and HCC827/AR cell lines and then tested its impact on induction of apoptosis by osimertinib and PF429242 combination. We found that the combination significantly enhanced apoptosis in the PC-9 parental cell line, as evidenced by increased cleavage of caspase-3 and PARP (Fig. 7G) and annexin V-positive populations (Fig. 7H), but had minimal or undetectable effect in all Bim-KO PC-9 cell lines (Figs. 7G and 7H). Similar results were also generated in HCC827/AR-Bim KO cell lines (Figs. 7I and 7J). Together, these findings indicate that the combination of osimertinib with SREBP1 inhibition enhances Bim-dependent apoptosis in osimertinib-resistant NSCLC cells.

Discussion

Our ultimate goal is to develop effective and clinically deliverable therapeutic strategies for overcoming acquired resistance to osimertinib and other third generation EGFR-TKIs. To achieve this goal, we need to fully understand the molecular mechanisms by which osimertinib exerts its anticancer activity against sensitive NSCLCs with EGFR activating mutations. The intriguing finding in this study is that osimertinib effectively decreased the levels of mSREBP1, ACC and FASN and suppressed intracellular lipid metabolism in sensitive EGFRm NSCLC cells, but not in cell lines with acquired resistance to osimertinib, strongly suggesting the possible involvement of the SREBP1/ACC/FASN axis and lipid metabolism modulation in osimertinib-based targeted therapy of lung cancer and the development of acquired resistance to osimertinib. Importantly, direct inhibition of SREBP1 using both genetic and pharmacological approaches in osimertinib-resistant cells and tumors restored the sensitivity of these resistant cells and tumors to osimertinib-treatment, whereas enforced expression of ectopic SREBP1 in the sensitive EGFRm NSCLC cells compromised osimertinib's ability to decrease cell survival and induce apoptosis. These findings strongly support the notion that suppression of the SREBP1/ACC/FASN axis and lipid metabolism is a critical mechanism accounting for therapeutic efficacy of osimertinib against EGFRm NSCLCs. Therefore, the findings in this study have established a novel and robust connection between the modulation of mSREBP1 stability including its mediated lipid metabolism and osimertinib-based therapy of EGFRm NSCLCs. This mechanism can also be applied to other third generation EGFR-TKIs because EGF816 and CO1686, two

other third generation EGFR-TKIs, effectively reduced the levels of mSREBP1, ACC and FASN in EGFRm NSCLC cells as well.

Although EGFRm NSCLC cells were initially sensitive to osimertinib, displaying suppression of the mSREBP1/ACC/FASN axis and its regulated lipid metabolism, they lose response to or become resistant to osimertinib modulation of this axis and lipid metabolism, likely due to the establishment of unknown bypass mechanisms or pathway or metabolism reprogramming. Intriguingly, we observed a rebound upregulation of the mSREBP1/ACC/FASN axis and lipid metabolism in EGFRm NSCLC cells with acquired resistance to osimertinib, although the underlying mechanisms are unclear. This rebound upregulation of the mSREBP1/ACC/FASN axis can be considered a prediction of development of acquired resistance to osimertinib or EGFR-TKIs, whereas the early suppression of this axis and its mediated lipid metabolism is a sign of patient response to treatment.

Findings in this study clearly suggest the critical role of SREBP1 elevation in emergence of acquired resistance to osimertinib and also provide compelling preclinical support and scientific rationale for directly targeting SREBP1 to overcome acquired resistance to osimertinib and possibly other third generation EGFR-TKIs. Currently, there are no SREBP1 inhibitors available or being tested in the clinic. Our findings thus warrant the development of specific and safe SREBP1 inhibitors, which can be used to overcome acquired resistance to osimertinib and possibly other third generation EGFR-TKIs. These inhibitors, when combined with osimertinib, may be also effective in treating the small proportion of EGFRm NSCLC patients who do not respond to osimertinib monotherapy. Given that sustained suppression of the SREBP1/ACC/FASN axis and its regulated lipid metabolisms is tightly coupled to therapeutic efficacy of osimertinib, early intervention in targeting this axis, such as using a SREBP1 inhibitor, may have potential impact on delaying or preventing the emergence of acquired resistance to osimertinib or other third generation EGFR-TKIs. Studies in this direction may be of benefit.

In relation to our current finding, it was previously shown that FASN expression is elevated in gefitinib-resistant EGFRm NSCLC cells[18] and inhibition of FASN with different inhibitors combined with gefitinib effectively suppressed the growth of gefitinib-resistant cells and tumors[18, 19]. Another recent study shows that glycerol kinase 5, a rate-limiting enzyme converting glycerol to glycerol 3-phosphate, confers gefitinib resistance through activating SREBP1/stearoyl-CoA-desaturase 1 (SCD1) axis and inhibition of SCD1 reverses gefitinib resistance[20]. Moreover, SREBP1 inhibition increased gefitinib sensitivity *in vitro* and *in vivo*[21]. Unfortunately, the results in this study were primarily generated in A549, a NSCLC cell line with WT EGFR, without studying EGFR-TKI acquired resistance. Nonetheless, these studies together with our current study have strongly suggested the potential of targeting the SREBP1/ACC/FASN in overcoming acquired resistance to EGFR-TKIs.

The rationale leading us to identify the novel connection between osimertinib and suppression of SREBP1/lipid metabolism came from our previous finding that mTORC2 positively regulates lipid metabolism through stabilizing mSREBP1[16] and current finding that osimertinib inhibits mTORC2 signaling. Since this study focuses on demonstrating

the modulation of SREBP1/lipid metabolism during osimertinib-based targeted therapy of EGFRm NSCLCs, we have not been able to elucidate how osimertinib inhibits mTORC2 signaling; this is our ongoing work. In agreement with our previous finding that mTORC2 stabilizes mSREBP1 through negative regulation of GSK3/FBXW7-mediated protein degradation[16], we have demonstrated that osimertinib facilitates GSK3/FBXW7-medaited proteasomal degradation of mSREBP1, decreasing mSREBP1 levels in EGFRm NSCLC cells.

Induction of Bim-dependent apoptosis is a key mechanism accounting for the therapeutic activity of osimertinib and other third generation EGFR-TKIs against EGFRm NSCLC, including overcoming acquired resistance as we demonstrated previously[13]. In this study, we have also demonstrated that SREBP1 inhibition combined with osimertinib enhances Bim-dependent apoptosis. Interestingly, this combination enhanced elevation of Mcl-1 levels while elevating Bim levels in these osimertinib-resistant cell lines; this modulation of Mcl-1 is different from that induced by osimertinib combined with MEK or ERK inhibition, which often enhances Mcl-1 reduction while elevating Bim levels[13, 22]. Nonetheless, the potential inhibitory effect caused by Mcl-1 elevation can be overridden by enhanced elevation of Bim because SREBP1 inhibition plus osimertinib clearly enhances Bim-dependent apoptosis in osimertinib-resistant cells. The current study is unable to address how SREBP1 suppression leads to Bim and Mcl-1 elevation, but our findings warrant future study toward this direction.

Materials and Methods

Reagents.

The SREBP1 inhibitors, PF429242 and betulin, were purchased from Sigma Aldrich (St. Louis, MO) and Merck (Kenilworth, NJ), respectively. SREBP1 antibody was purchased from BD Biosciences (#557036; San Jose, CA). FASN antibody was purchased from Santa Cruz Biotechnology (SC-55580; Santa Cruz, CA). ACC antibody was purchased from Cell Signaling Technology, Inc (#3662; Beverly, MA). Nile Red (N1142), DAPI (62248) and the secondary antibodies, Alexa Fluor 488-Donkey anti-mouse (A32766) and Alexa Fluor 568-Donkey anti-rabbit (A10042) were purchased from Thermo Fisher Scientific (Waltham, MA). Other reagents and antibodies were the same as described previously[13, 23].

Cell lines and cell culture.

All cell lines including PC-9/AR/Bim-KO and HCC827/AR/Bim-KO used in this study were described previously[13, 24, 25]. The cell lines that stably express ectopic SREBP1 were established with infection of lentiviruses carrying human SREBF1 gene that encodes SREBP1 followed by kanamycin selection. SREBF1 and vector control lentiviruses were made from SREBF1 lentivial plasmid (Cat#454470610195) and matched vector pLenti-GIII-CMV, respectively, which were purchased from Applied Biological Materials (abm) Inc. (Richmond, BC V6V 2J5, Canada), as instructed by the manufacturer. These cell lines have not been authenticated recently. All cell lines were cultured in RPIM1640 medium supplemented with 5% FBS at 37°C in 5% CO_2 humidified air.

Cell survival assay.

Cells numbers in 96-well plates were measured by sulforhodamine B (SRB) assay as previously described[26]. Combination Index (CI) for drug interaction was calculated with the CompuSyn software (ComboSyn, Inc; Paramus, NJ).

Colony formation assay.

The procedure for this assay in 12-well plates were the same as described previously[13].

Detection of apoptosis.

Apoptosis was detected using the annexin V/7-AAD apoptosis detection Kit (BD Biosciences; San Jose, CA) according to the manufacturer's instructions. Protein cleavage as an additional indicator of apoptosis was evaluated by Western blotting.

Western blot analysis.

Preparation of whole-cell protein lysates and Western blotting were the same as described previously[27]. Protein band intensities were quantified by NIH ImageJ software.

Gene knockdown with siRNA or shRNA.

SREBP1 siRNA (sc-36557) was purchased from Santa Cruz Biotechnology. The procedures used for transfection, as well as the details of the scrambled control, FBXW7 and GSK3 siRNAs, were described previously[16]. Lentiviral SREBP1 and FBXW7 shRNAs were generously provided by Dr. Deliang Guo (The Ohio State Medical Center, Columbus, OH)[28] and Dr. Wenyi Wei (Beth Israel Deaconess Medical Center and Harvard Medical School, Boston, MA)[29], respectively.

Animal xenografts and treatment.

All animal experiments were approved by the Institutional Animal Care and Use Committee (IACUC) of Emory University. In brief, the tested cells were subcutaneously injected into NU/NU nude mice (2×10^6/animal). Treatments included vehicle control, osimertinib (5 mg/kg/day, og), PF429242 (25 mg/kg/day, ip) and their combination. Tumor size measurement and others were the same as described previously[13].

Statistical analysis.

Statistical differences were determined by two-sided unpaired Student's t-test. Results are presented as means ± SDs or SEs. All statistical analyses were conducted using Graphpad Prism 8.0 software. P values less than 0.05 were considered statistically significant. All data were repeated at least once or in different cell lines or models.

For other related methods, please see supplementary Materials and Methods section.

Supplementary Material

Refer to Web version on PubMed Central for supplementary material.

Acknowledgements

We are thankful to Dr. Dongsheng Wang and Mr. Guojing Zhang in our department for helping us with animal experiments, to Dr. Teng Wang and Dr. Dong Hua (Affiliated Hospital of Jiangnan University) for providing us with clinical samples, to Dr. Peng Zhang (Longgang E.N.T. Hospital & Shenzhen Key Laboratory of E.N.T.) for staining the patients' samples, and to Drs. Deliang Guo and Wenyi Wei for providing some shRNAs. We are also grateful to Dr. Anthea Hammond in our department for editing the manuscript.

This work was supported by the NIH/NCI R01 CA223220 (to S-Y.S.), R01 CA245386 (to S-Y.S.), UG1 CA233259 (to S.S.R.) and lung cancer SPORE P50 CA217691 DRP award (to S-YS) and Emory University Winship Cancer Institute lung cancer pilot funds (to S-Y.S)

DY is a visiting medical student participating in the Xiangya-Emory Visiting Medical Student Program. S.S.R., T.K.O. and S-Y.S. are Georgia Research Alliance Distinguished Cancer Scientists.

Abbreviations:

SREBP1	Sterol regulatory element-binding protein 1
mSREBP1	matured SREBP1
NSCLC	non-small cell lung cancer
EGFR	epidermal growth factor receptor
EGFRm	EGFR mutant
EGFR-TKIs	EGFR-tyrosine kinase inhibitors
FASN	fatty-acid synthase
ACC	acetyl-CoA carboxylase
mTORC2	mTOR complex 2
WT	wild-type
IF	immunofluorescence
CHX	cycloheximide
IHC	immunohistochemistry
siRNA	small-interfering RNA
shRNA	short-hairpin RNA
CI	combination index

References

1. Malvezzi M, Carioli G, Bertuccio P, Boffetta P, Levi F, La Vecchia C et al. European cancer mortality predictions for the year 2017, with focus on lung cancer. Annals of oncology : official journal of the European Society for Medical Oncology / ESMO 2017; 28: 1117–1123.
2. Siegel RL, Miller KD, Jemal A. Cancer statistics, 2018 2018; 68: 7–30.

3. Recondo G, Facchinetti F, Olaussen KA, Besse B, Friboulet L. Making the first move in EGFR-driven or ALK-driven NSCLC: first-generation or next-generation TKI? Nat Rev Clin Oncol 2018; 15: 694–708. [PubMed: 30108370]
4. Soria JC, Ohe Y, Vansteenkiste J, Reungwetwattana T, Chewaskulyong B, Lee KH et al. Osimertinib in Untreated EGFR-Mutated Advanced Non-Small-Cell Lung Cancer. N Engl J Med 2018; 378: 113–125. [PubMed: 29151359]
5. Röhrig F, Schulze A. The multifaceted roles of fatty acid synthesis in cancer. Nature reviews Cancer 2016; 16: 732–749. [PubMed: 27658529]
6. Merino Salvador M, Gómez de Cedrón M, Moreno Rubio J, Falagán Martínez S, Sánchez Martínez R, Casado E et al. Lipid metabolism and lung cancer. Critical reviews in oncology/hematology 2017; 112: 31–40. [PubMed: 28325263]
7. Guo D, Reinitz F, Youssef M, Hong C, Nathanson D, Akhavan D et al. An LXR agonist promotes glioblastoma cell death through inhibition of an EGFR/AKT/SREBP-1/LDLR-dependent pathway. Cancer discovery 2011; 1: 442–456. [PubMed: 22059152]
8. Yue S, Li J, Lee SY, Lee HJ, Shao T, Song B et al. Cholesteryl ester accumulation induced by PTEN loss and PI3K/AKT activation underlies human prostate cancer aggressiveness. Cell metabolism 2014; 19: 393–406. [PubMed: 24606897]
9. Guo D, Bell EH, Mischel P, Chakravarti A. Targeting SREBP-1-driven lipid metabolism to treat cancer. Current pharmaceutical design 2014; 20: 2619–2626. [PubMed: 23859617]
10. Cheng X, Li J, Guo D. SCAP/SREBPs are Central Players in Lipid Metabolism and Novel Metabolic Targets in Cancer Therapy. Current topics in medicinal chemistry 2018; 18: 484–493. [PubMed: 29788888]
11. Horton JD, Goldstein JL, Brown MS. SREBPs: activators of the complete program of cholesterol and fatty acid synthesis in the liver. J Clin Invest 2002; 109: 1125–1131. [PubMed: 11994399]
12. Guo D, Prins RM, Dang J, Kuga D, Iwanami A, Soto H et al. EGFR signaling through an Akt-SREBP-1-dependent, rapamycin-resistant pathway sensitizes glioblastomas to antilipogenic therapy. Sci Signal 2009; 2: ra82. [PubMed: 20009104]
13. Shi P, Oh YT, Deng L, Zhang G, Qian G, Zhang S et al. Overcoming Acquired Resistance to AZD9291, A Third-Generation EGFR Inhibitor, through Modulation of MEK/ERK-Dependent Bim and Mcl-1 Degradation. Clin Cancer Res 2017; 23: 6567–6579. [PubMed: 28765329]
14. Wee P, Wang Z. Epidermal Growth Factor Receptor Cell Proliferation Signaling Pathways. Cancers 2017; 9:52.
15. Oh WJ, Jacinto E. mTOR complex 2 signaling and functions. Cell Cycle 2011; 10: 2305–2316. [PubMed: 21670596]
16. Li S, Oh YT, Yue P, Khuri FR, Sun SY. Inhibition of mTOR complex 2 induces GSK3/FBXW7-dependent degradation of sterol regulatory element-binding protein 1 (SREBP1) and suppresses lipogenesis in cancer cells. Oncogene 2016; 35: 642–650. [PubMed: 25893295]
17. Hagiwara A, Cornu M, Cybulski N, Polak P, Betz C, Trapani F et al. Hepatic mTORC2 activates glycolysis and lipogenesis through Akt, glucokinase, and SREBP1c. Cell metabolism 2012; 15: 725–738. [PubMed: 22521878]
18. Ali A, Levantini E, Teo JT, Goggi J, Clohessy JG, Wu CS et al. Fatty acid synthase mediates EGFR palmitoylation in EGFR mutated non-small cell lung cancer. EMBO molecular medicine 2018; 10: e8313. [PubMed: 29449326]
19. Polonio-Alcala E, Palomeras S, Torres-Oteros D, Relat J, Planas M, Feliu L et al. Fatty Acid Synthase Inhibitor G28 Shows Anticancer Activity in EGFR Tyrosine Kinase Inhibitor Resistant Lung Adenocarcinoma Models. Cancers 2020; 12:1283.
20. Zhou J, Qu G, Zhang G, Wu Z, Liu J, Yang D et al. Glycerol kinase 5 confers gefitinib resistance through SREBP1/SCD1 signaling pathway. Journal of experimental & clinical cancer research : CR 2019; 38: 96. [PubMed: 30791926]
21. Li J, Yan H, Zhao L, Jia W, Yang H, Liu L et al. Inhibition of SREBP increases gefitinib sensitivity in non-small cell lung cancer cells. Oncotarget 2016; 7: 52392–52403. [PubMed: 27447558]
22. Li Y, Zang H, Qian G, Owonikoko TK, Ramalingam SR. ERK inhibition effectively overcomes acquired resistance of epidermal growth factor receptor-mutant non-small cell lung cancer cells to osimertinib 2020; 126: 1339–1350.

23. Zhao W, Yu D, Chen Z, Yao W, Yang J, Ramalingam SS et al. Inhibition of MEK5/ERK5 signaling overcomes acquired resistance to the third generation EGFR inhibitor, osimertinib, via enhancing Bim-dependent apoptosis. Cancer Lett 2021; 519: 141–149. [PubMed: 34245854]

24. Zang H, Qian G, Arbiser J, Owonikoko TK, Ramalingam SS, Fan S et al. Overcoming acquired resistance of EGFR-mutant NSCLC cells to the third generation EGFR inhibitor, osimertinib, with the natural product honokiol. Mol Oncol 2020; 14: 882–895. [PubMed: 32003107]

25. Yu D, Li Y, Sun KD, Gu J, Chen Z, Owonikoko TK et al. The novel MET inhibitor, HQP8361, possesses single agent activity and enhances therapeutic efficacy of AZD9291 (osimertinib) against AZD9291-resistant NSCLC cells with activated MET. Am J Cancer Res 2020; 10: 3316–3327. [PubMed: 33163272]

26. Sun SY, Yue P, Dawson MI, Shroot B, Michel S, Lamph WW et al. Differential effects of synthetic nuclear retinoid receptor-selective retinoids on the growth of human non-small cell lung carcinoma cells. Cancer Res 1997; 57: 4931–4939. [PubMed: 9354460]

27. Yao W, Yue P, Zhang G, Owonikoko TK, Khuri FR, Sun SY. Enhancing therapeutic efficacy of the MEK inhibitor, MEK162, by blocking autophagy or inhibiting PI3K/Akt signaling in human lung cancer cells. Cancer Lett 2015; 364: 70–78. [PubMed: 25937299]

28. Geng F, Cheng X, Wu X, Yoo JY, Cheng C, Guo JY et al. Inhibition of SOAT1 Suppresses Glioblastoma Growth via Blocking SREBP-1-Mediated Lipogenesis. Clinical cancer research : an official journal of the American Association for Cancer Research 2016; 22: 5337–5348. [PubMed: 27281560]

29. Takada M, Zhang W, Suzuki A, Kuroda TS, Yu Z, Inuzuka H et al. FBW7 Loss Promotes Chromosomal Instability and Tumorigenesis via Cyclin E1/CDK2-Mediated Phosphorylation of CENP-A. Cancer research 2017; 77: 4881–4893. [PubMed: 28760857]

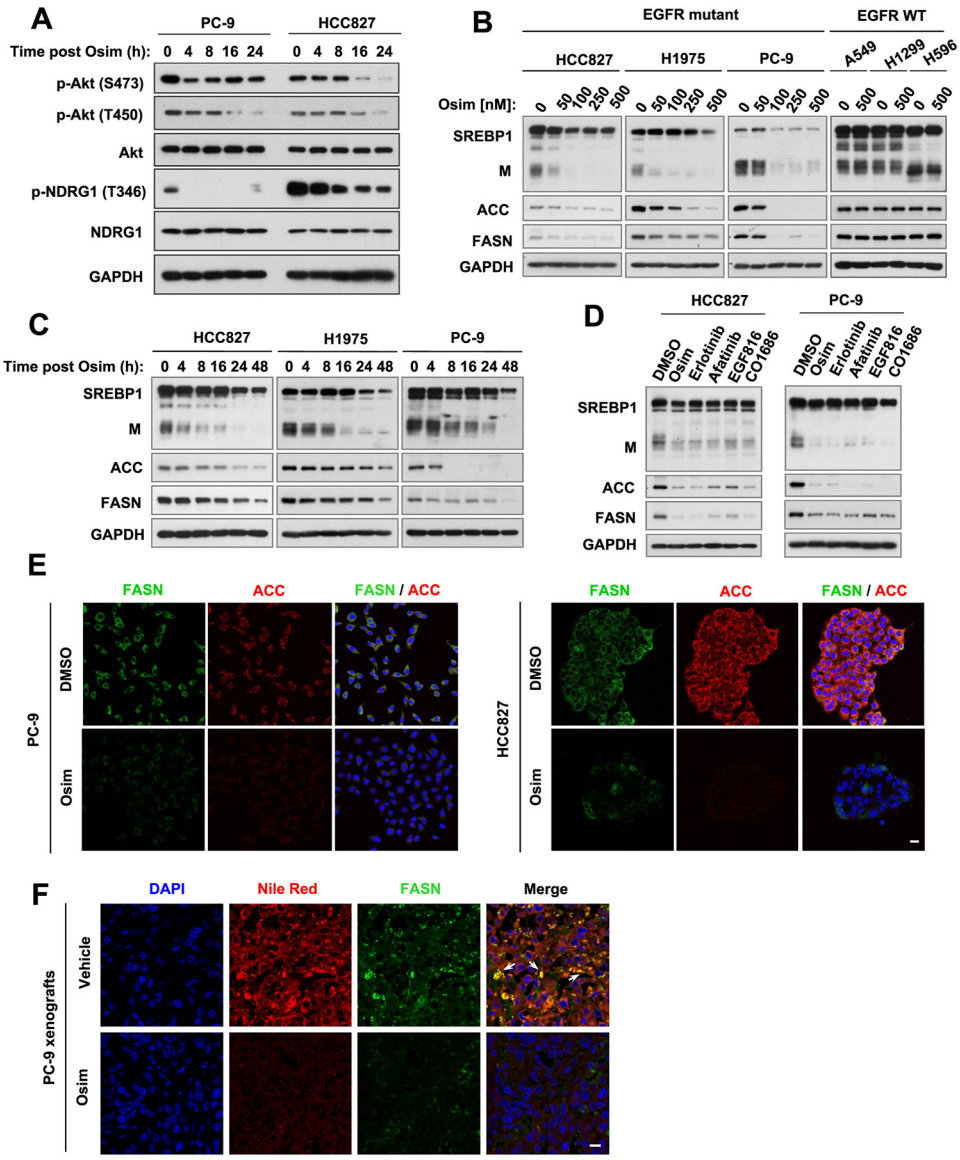

Figure 1. Osimertinib inhibits mTORC2 signaling and decreases mSREBP1 levels in EGFRm NSCLC cells accompanied with reduction of ACC and FASN.

A-D, The given cell lines were treated with 200 nM osimertinib for different times as indicated (**A** and ***C***), with different concentrations of osimertinib for 24 h (***B***), or with the indicated EGFR-TKIs at 200 nM for 24 h (***D***). Western blotting was used to detect the indicated proteins in whole-cell protein lysates prepared from these treatments. M, mature form. ***E***, Representative IF images showing the FASN (green) and ACC (red) expression in PC-9 and HCC827 cells exposed to 100 nM osimertinib for 24 h. Scale bars, 25 μm. ***F***, Representative IF images showing lipid droplets after Nile Red staining and FASN expression in PC-9 xenografts receiving vehicle or osimertinib treatment, respectively. The arrows indicate the co-localization of Nile Red (Red) and FASN (Green). Scale bars, 25 μm.

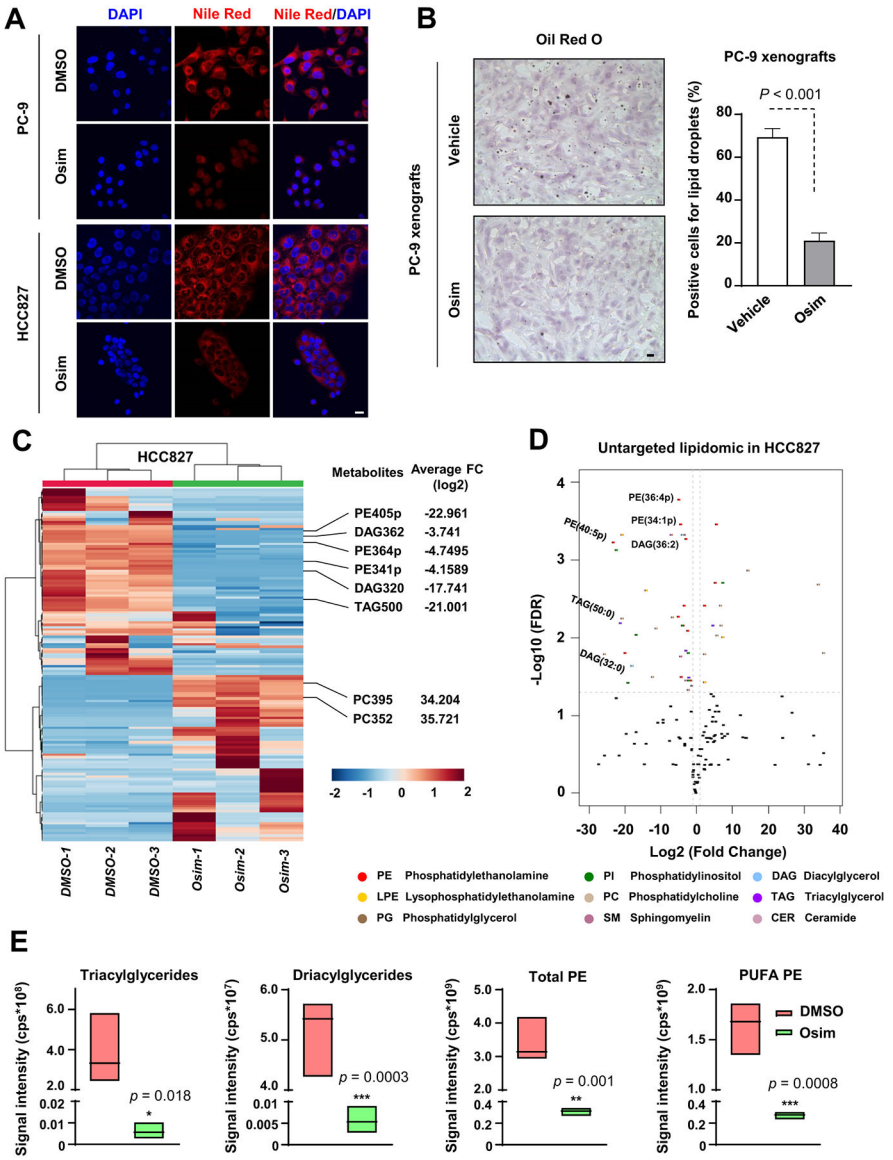

Figure 2. Osimertinib effectively suppresses SREBP1-regulated lipid metabolism in EGFRm NSCLC cells.

A, Representative IF images showing lipid droplets after Nile Red staining in PC-9 and HCC827 cells exposed to DMSO or 100 nM osimertinib for 24 h. Scale bars, 25 μm. ***B***, Oil Red O staining showing significant decrease of lipid droplets in PC-9 xenografts treated with osimertinib in comparison with vehicle control tumors. Left panels: representative images of Oil Red O staining; right panels: positive cells for lipid droplets. Scale bars: 50 μm. ***C***, Cluster analysis of lipidomic results in HCC827 cells treated with DMSO vs. osimertinib. Representative lipid species names and average fold changes are noted. ***D***, Significantly changed lipid species ($P < 0.05$) between DMSO- and osimertinib-treated HCC827 cells are shown in volcano plots with log2 (fold change) on the x-axis and −log10 (FDR) on the y-axis and are marked with colored dots based on their lipid classes. Representative significantly changed PE, TAG and DAG are labeled with their number of carbons and unsaturation contained on the fatty acid moiety. Different lipid classes with their colors

are shown in the legend at bottom. N = 3 independent replicates per hairpin. FDR, false discovery rate. ***E***, Box plots showing that the lipid classes of TAG, DAG, PE, especially PUFA PE, were significantly reduced when HCC827 cells were treated with 200 nM osimertinib for 24 h.

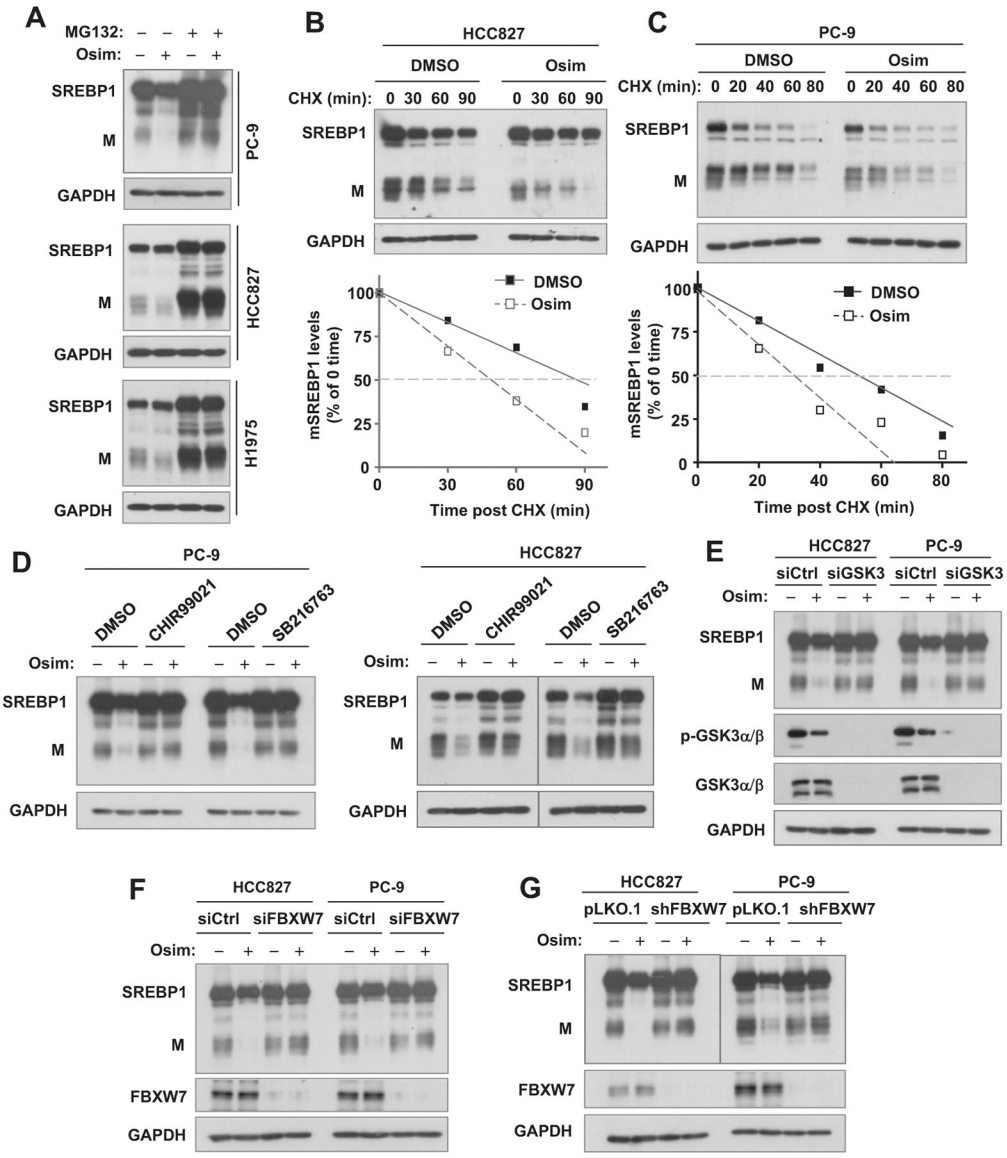

Figure 3. Osimertinib reduces mSREBP1 levels through facilitating GSK3/FBXW7-mediated mSREBP1 degradation.

A, The indicated EGFR mutant cell lines were pre-treated with 10 μM MG132 for 30 min, then co-treated with DMSO or 200 nM osimertinib for another 4 h. ***B*** and ***C***, Both HCC827 and PC-9 cells were treated with 200 nM osimertinib for 16 h followed by the addition of 10 μg/ml CHX and then cells were harvested at the indicated times. ***D***, PC-9 and HCC827 cells were pre-treated with 10 μM CHIR99021 or SB216763 for 30 min and then co-treated with 200 nM osimertinib for an additional 16 h. ***E*** and ***F***, PC-9 and HCC827 cells were transfected with the scrambled control, GSK3 (E) or FBXW7 (F) siRNA for 48 h followed by treatment with 200 nM osimertinib for another 24 h. ***G***, PC-9 and HCC827 cell lines expressing pLKO.1 or shFBXW7 were exposed to 200 nM osimertinib for 24 h. Whole cell-protein lysates were prepared from the aforementioned treatments for the detection of the specified proteins with Western blotting. Band intensities were quantified with NIH Image J software **(*B* and *C*)**.

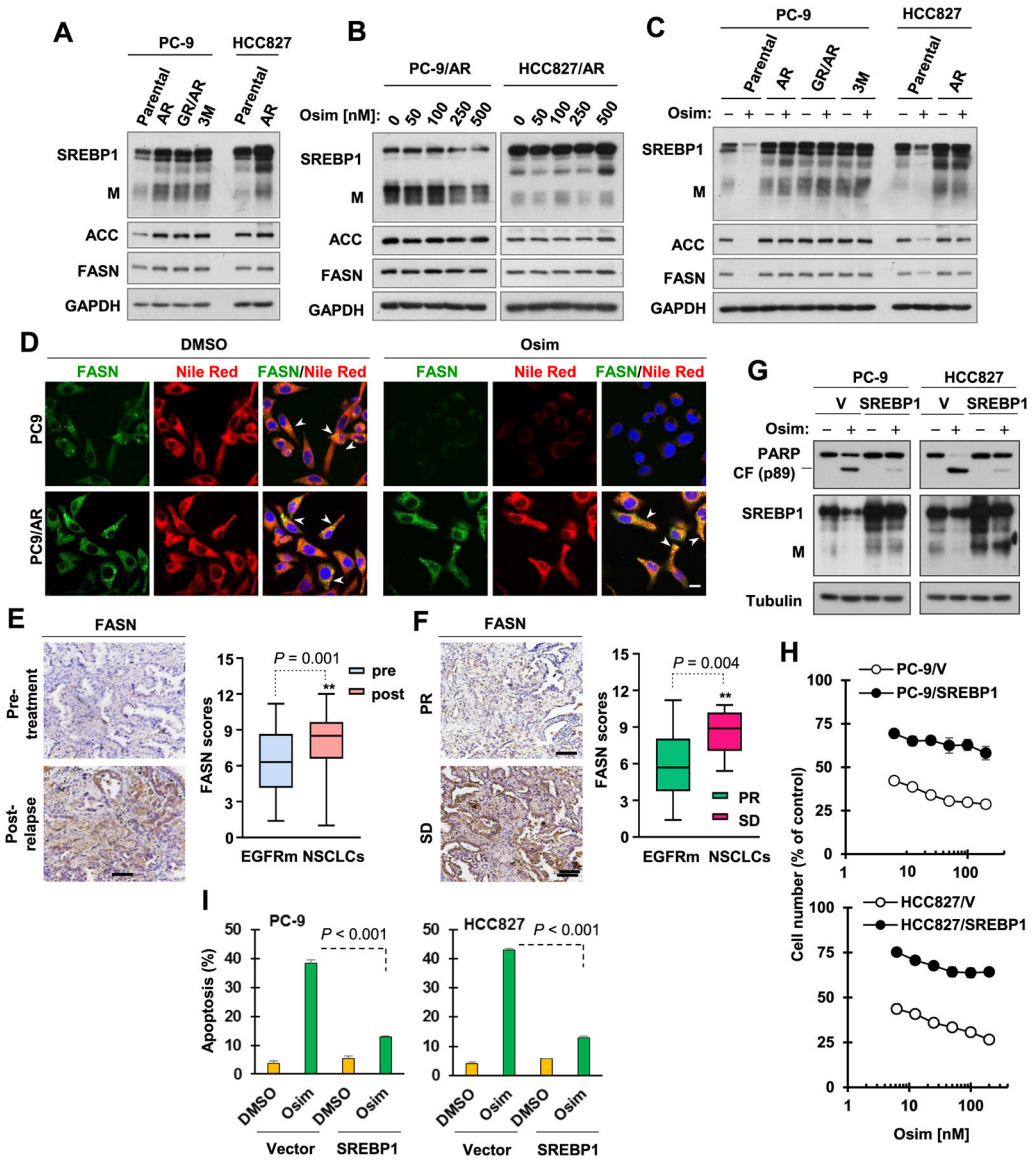

Figure 4. EGFRm NSCLC cells and tissues with acquired resistance to osimertinib or other EGFR-TKIs possess elevated levels of mSREBP1 and/or FASN, which are resistant to osimertinib modulation, and enforced expression of ectopic SREBP1 in sensitive EGFRm NSCLC cells confers resistance to osimertinib.

A-C, Western blot analysis showing the basal levels of SREBP1, ACC and FASN in the indicated cell lines (***A***), the levels of SREBP1, ACC and FASN in the indicated cells treated with different concentrations of osimertinib (Osim) as indicated for 24 h (***B***), and the levels of SREBP1, ACC and FASN in the given cell lines exposed to 200 nM osimertinib for 24 h (***C***). ***D***, Nile Red assay and FASN expression in the indicated cell lines exposed to 200 nM osimertinib for 24 h were conducted with IF staining. Scale bars, 25 μm. ***E***, Representative images and summary data from IHC staining of FASN in paired tissues from patients before and after relapse to the first-generation EGFR-TKI treatment were presented (n=46). ***F***, FASN expression in patients with stable disease (SD; n =8) and patients with partial response (PR; n =38) was stained with IHC. Scale bars, 50 μm. ***G*** and ***I***, The indicated

cell lines were exposed to DMSO or 200 nM for 24 h. The tested proteins were detected with Western blotting (***G***) and apoptotic cells were detected with annexin V staining/flow cytometry (***I***). The data represent means ± SDs of duplicate treatments. ***H***, The given cell lines in 96-well plates were treated with different concentration of osimertinib as indicated for 48 h. Cell numbers were measured with the SRB assay. The data are means ± SDs of four replicate determinations.

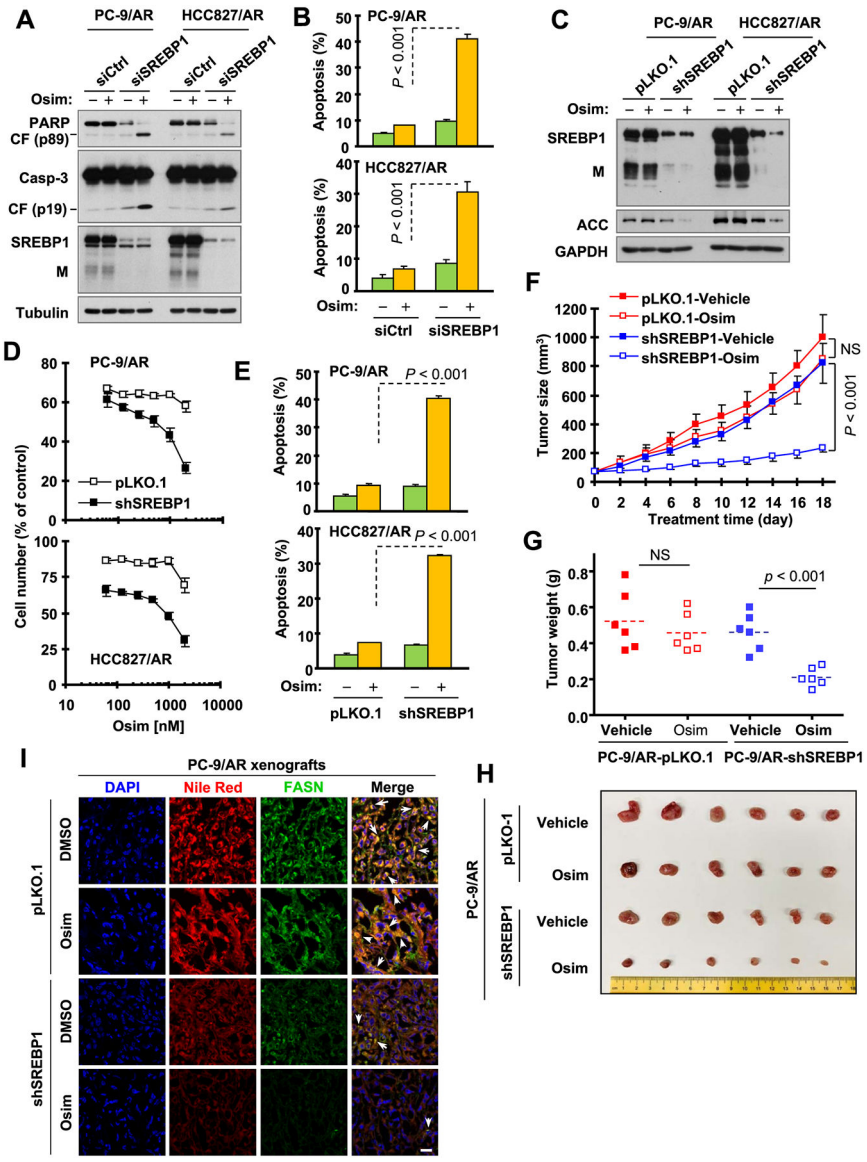

Figure 5. Genetic knockdown of SREBP1 reverses osimertinib resistance *in vitro* and *in vivo*.

A and ***B***, PC-9/AR and HCC827/AR cells were transfected with scrambled control or SREBP1 siRNA for 48 h and then exposed to 250 nM osimertinib for 48 h (***A***) or 72 h (***B***). Western blotting was used to detect the levels of PARP, caspase-3 and SREBP1 (***A***) and flow cytometry was used to detect annexin V-positive cells (***B***). The data represent means ± SDs of duplicate determinations. CF, cleavage form. ***C***, The given cell lines expressing pLKO.1 or shSREBP1 were treated with DMSO or 250 nM osimertinib for 48 h and then harvested for preparation of whole-cell protein lysates and subsequent Western blotting to detect the specified proteins. ***D*** and ***E***, The indicated cell lines were exposed to different concentrations of osimertinib (***D***) or 250 nM osimertinib (***E***) for 3 days. Cell numbers were measured by the SRB assay (***D***) and apoptosis was detected with flow cytometry for annexin V-positive cells (***E***). The data represent means ± SDs of four replicate determinations (***D***) or duplicate treatments (***E***). ***F-H***, PC-9/AR-pLKO.1 and PC-9/AR-shSREBP1 tumors were treated with

vehicle or osimertinib (5 mg/kg/day, og) for 3 weeks. Corresponding tumor growth curves were measured at the indicated time points (***F***). Tumor weights were also measured (***G***) and photographed (***H***) at the end of treatments. The data in each group are means ± SDs of 6 tumors from 6 mice. NS, not significant. ***I***, IF staining for FASN (green) and lipid droplets of Nile Red (red) in the indicated tumor sections. Scale bars: 25 μm.

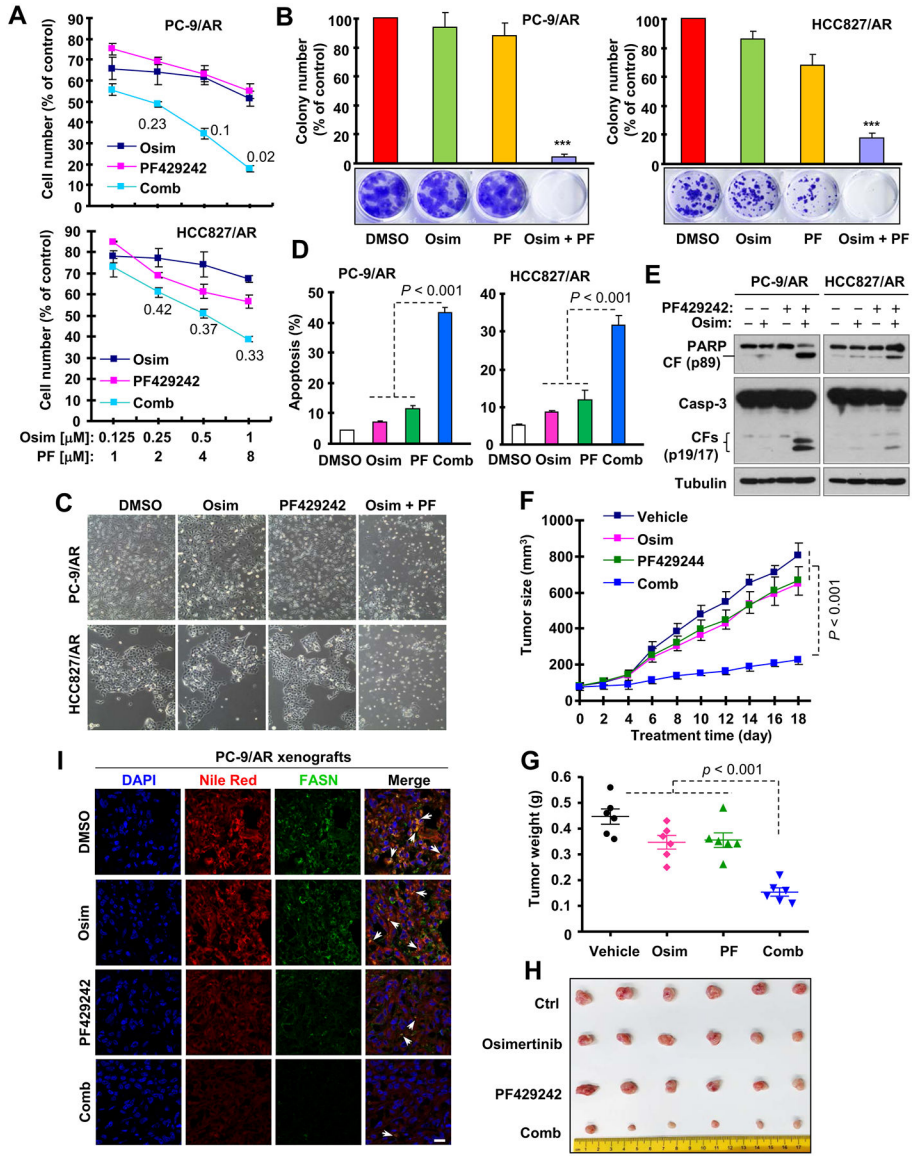

Figure 6. Chemical inhibition of SREBP1 combined with osimertinib synergistically decreases survival with enhanced apoptosis of osimertinib-resistant NSCLC cells and overcomes osimertinib resistance *in vivo*.

A, PC-9/AR and HCC827/AR cells were exposed to varied concentrations of osimertinib alone, PF429242 (PF) alone or their respective combinations for 3 days. Cell numbers were the estimated with the SRB assay. The numbers in the graphs are CIs for different combinations and the data represent means ± SDs of four replicate determinations. ***B***, PC-9/AR and HCC827/AR cells seeded in 12-well plates were treated with 50 nM osimertinib, 100 nM PF429242 or their combination; these treatments were repeated with fresh medium every 3 days. After 10 days, the cells were the fixed and stained with crystal violet dye. Columns are means ± SDs of triplicate determinations. ***C-E***, The indicated cell lines were exposed to 250 nM osimertinib, 5 μM PF429242 or their combinations for 72 h (***C*** and ***D***) or 48 h (***E***). Photos were then taken to show representative images of cellular morphological changes (***C***). Apoptosis was detected with flow cytometry for annexin V-

positive cells (***D***) or Western blotting for the cleavage of PARP and caspase-3 cleavage (***E***). ***F-H***, PC-9/AR cells grown in NU/NU mice as xenografted tumors were treated with vehicle, osimertinib alone (5 mg/kg/day, og), PF429242 alone (25 mg/kg/day, ip) or the combination of osimertinib with PF429242. Tumor sizes were measured at the indicated time points (***F***). At the end of treatment, tumors in each group were also weighed (***G***) and photographed (***H***). The data in each group are means ± SDs of 6 tumors from 6 mice. NS, not significant. ***I***, Representative IF images showing lipid droplets of Nile Red staining and FASN expression in each group of xenografts. Scale bars, 25 μm. Comb, combination.

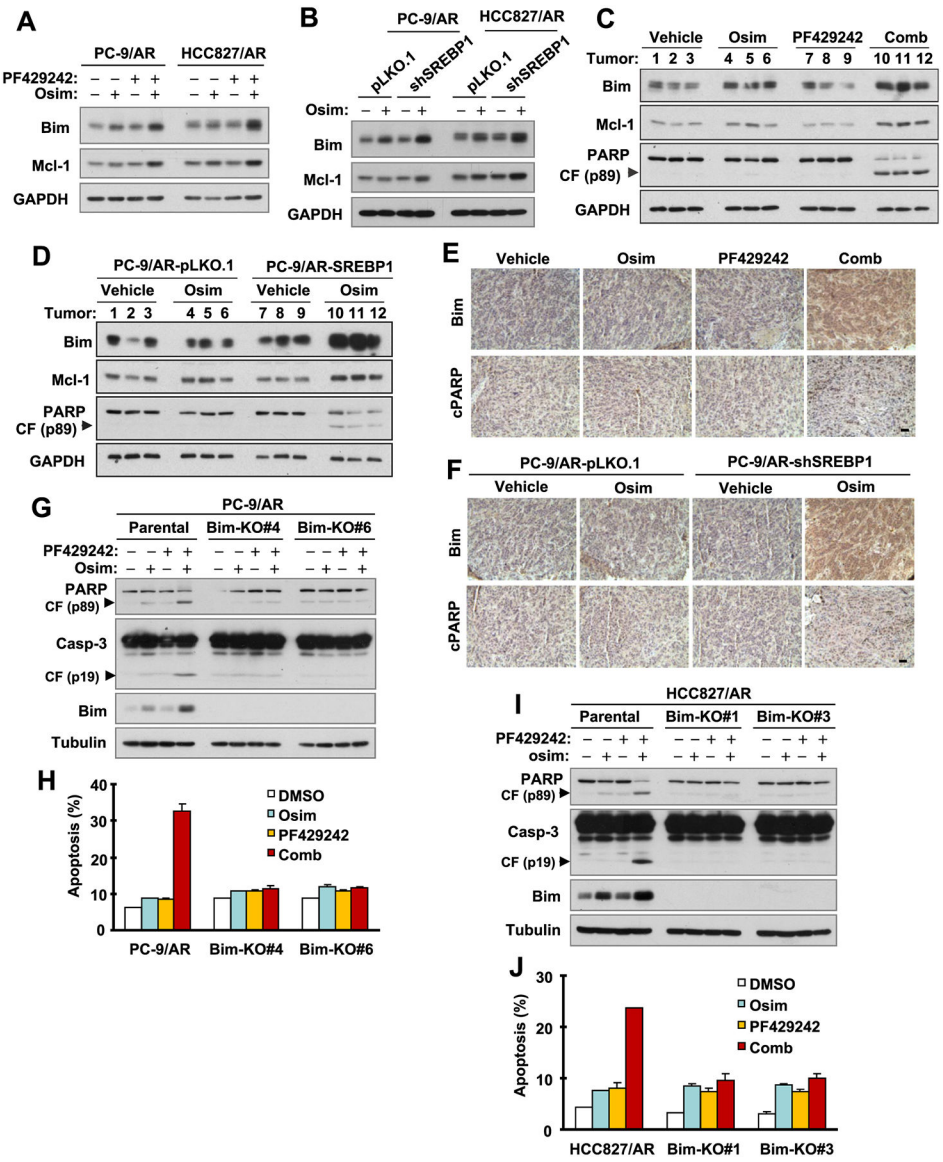

Figure 7. Osimertinib combined with SREBP1 inhibition enhances Bim and Mcl-1 levels and augments Bim-dependent apoptosis in osimertinib-resistant cells.

A and ***B***, The indicated cell lines were treated with 250 nM osimertinib, 5 μM PF429242 or their combinations (***A***) or with DMSO or 250 nM osimertinib (***B***) for 16 h. Western blotting was used to detect the given proteins. ***C*** and ***D***, Whole-tumor protein lysates were prepared from three tumors randomly in each group as presented in figures 5 and 6 to detect the indicated proteins by Western blotting. ***E*** and ***F***, IHC staining of Bim, Mcl-1 and cleaved PARP in sections of indicated tumor xenografts. Scale bars: 50 μm. ***G-J***, Both PC-9/AR and HCC827/AR cell lines and their derived Bim knockout cell lines were treated with 250 nM osimertinib, 5 μM PF429242 or osimertinib plus PF429242 for 48 h and then harvested for Western blot analysis for the detection of specified proteins (***G*** and ***I***) and for flow cytometry to detect annexin V-positive cells (***H*** and ***J***).